ISSN 0027-1349, Moscow University Physics Bulletin, 2022, Vol. 77, No. 6, pp. 876–884. © Allerton Press, Inc., 2022.

BIOPHYSICS AND MEDICAL PHYSICS

An Investigation on Production Routes of ^{230}U Radioisotope Used in Targeted Alpha Therapy by Different Level Density Models

Hasan Özdoğan[1*], Mert Şekerci[2], Merve Cinoğlu Karaca[3], Murat Okutan[4], Bayram Demir[5], and Abdullah Kaplan[6]

[1]*Department of Medical Imaging Techniques, Vocational School of Health Services, Antalya Bilim University, 07190, Antalya, Turkey*

[2]*Department of Physics, Süleyman Demirel University, 32260, Isparta, Turkey*

[3]*University of Health Sciences Turkey, İstanbul Okmeydani Training and Research Hospital, Clinic of Nuclear Medicine, İstanbul, Turkey*

[4]*Division of Medical Physics, Istanbul University Oncology Institute, 34093, Istanbul, Turkey*

[5]*Department of Physics, İstanbul University, 34134, İstanbul, Turkey*

[6]*Department of Physics, Süleyman Demirel University, 32260, Isparta, Turkey*

Received July 08, 2021; revised March 07, 2022; accepted November 10, 2022

Abstract—Targeted alpha therapy (TAT) is an attractive therapeutic option in patients with multiple micrometastases. It offers many advantages, including easy administration, the ability to treat multiple lesions simultaneously and the possibility of combination with other therapeutic approaches for improved efficacy. The aim of this study is to investigate the optimum production route of ^{230}U, which is a promising TAT isotope, in cyclotrons. For this, ^{231}Pa$(p,2n)^{230}$U, ^{231}Pa$(d,3n)^{230}$U, ^{232}Th$(p,3n)^{230}$Pa and ^{232}Th$(d,4n)^{230}$Pa reactions cross–sections, total activity and reaction yield have been calculated by using different level density models of TALYS 1.95 code. It is possible to produce an ^{230}U activity of 53.491 mCi via on ^{231}Pa$(p,2n)^{230}$U direct route with 12.8 MeV protons at 1 mA current for 24 hours. After a 28 days waiting period required for undesirable product (^{231}U) activity to decrease sufficiently, this activity decreases to 21.4 mCi and by considering the average dose per patient as 0.5 mCi, these activities are enough for 43 patients. Besides, ^{231}Pa is already the target material in this direct production route and ^{231}Pa obtained from undesirable product ^{231}U can be stored and processed for re-use as the target material. In this way, a significant amount of source material can be recovered.

DOI: 10.3103/S0027134922060170

1. INTRODUCTION

In addition to surgery and chemotherapy applications preferred for cancer treatment, radiation therapy is also an important and frequently used option. While External Radiotherapy and Brachytherapy have been actively used in cancer treatment applications, recent breakthroughs have been made in the field of targeted internal radionuclide therapy (Targeted Therapies) that will become a very valuable and important option for the treatment of cancer. The first application of this treatment was Hyperthyroidism and thyroid cancer treatment with Iodine-131 (^{131}I) and it has already been performed for over 80 years [1, 2]. ^{131}I can be directly retained by the thyroid gland without binding to any biological agent. However, radionuclide such as Lutetium-177 (^{177}Lu), a beta emitter used in the treatment of neuroendocrine tumours, must be bound to a biological agent (such as DOTATOC, DOTATATE)[3].

In recent years, there has been an increasing interest in the targeted internal radionuclide therapy with alpha-emitting radioisotopes (TAT; Targeted Alpha Therapy). Neuroendocrine tumours [4], leukaemia [5] and Hodgkin lymphoma [6] can be shown as examples of some types of cancer that are known to use TAT applications in their treatments. It is a known fact that there are many important limitations in radiation therapy, and the most important of

*E-mail: hasan.ozdogan@antalya.edu.tr

these limitations is the risk of high dose irradiation of healthy tissues and organs. This situation emerges as the risk of irradiation of the organs in the radiation path, especially in the treatment applications performed with high doses in external radiotherapy. The energies of the alpha rays used in the TAT applications are around 6 MeV and their path length in tissue is around 40–100 micrometers. Since the radioactive isotope directly accumulates in the tumour and irradiates the tumour from the inside, TAT is a very promising and patient–friendly application in protecting healthy tissue.

Compared to the X- and beta rays; alpha particles linear energy transfer (LET) values are much higher (betas: 0.2 KeV/micrometer; alphas: 100 keV/micrometer) and their relative biological effectiveness (RBE) are about 20 times greater [7]. Moreover, the ability of alpha particles to kill cells by causing double-strand breaks is an important feature that makes them much more valuable than other beams in terms of causing more damage to targeted cancer cells. While it is enough to kill a cell with a few alpha particles to hit the cell, in the case of betas, 10^4 beta beams must cross the cell. In addition to all these advantages, since this cell killing mechanism of alpha rays does not rely on free radical formation, unlike beta rays, the possibility of a resistance mechanism to radiation therapy is eliminated [8].

The day–scale half–life of a TAT isotope is extremely important to prevent loss of activity during transport. In addition, a comparatively longer half–life is an advantageous factor in preventing radioactive contamination during the radiochemical process and the distribution of the radio-pharmaceutical in the body. Naturally, isotopes that emit the more alpha particles in the decay chain can be shown as the most ideal isotopes for the TAT applications. Although Uranium-230 (^{230}U) is not used for clinical purposes yet, it emerges as one of the rare TAT radioisotopes in which all desired requirements come together with its 20.8 days of half-life and other advantages. The decay chain of ^{230}U is ^{230}U (α, 20.8 days), ^{226}Th (α, 30.6 minutes), ^{222}Ra (α, 32.6 seconds), ^{218}Rn (α, 35 milliseconds), ^{214}Po (α, 164 microseconds), ^{210}Pb and the final product ^{210}Pb has a half-life of 22.3 years. Although the accumulation of ^{210}Pb in the blood is an important problem for the patients, due to the very low treatment doses applied in this treatment (maximum dose is 1 mCi ^{210}Pb for a 70 kg patients and it is nearly equal to 13 microgram ^{210}Pb), thus, the lead concentration in the blood per liter is far below the value allowed by WHO (10 microgram/liter) [9]. There are no beta rays on the decay chain of ^{230}U. Each decay is 100% alpha decay and a total of 5 alphas are emitted in these decay chain. Gamma rays with 84, 154, 158, 230, 235 keV energies emitted within the ^{230}U decay can be used for dosimetric imaging [10]. All these positive features of the ^{230}U make it an ideal alpha emitter for the TAT applications.

Actinium-225 (^{225}Ac) and Radium-223 (^{223}Ra) are nowadays routinely used in the clinics. Actinium-225 (^{225}Ac) is an alpha emitter with a half–life of 10.1 days. Five alphas and three betas are emitted in the decay chain until it decays to Bismuth-209 (^{209}Bi) [11]. Radium-223 (^{223}Ra) is an isotope of radium with an 11.4 day half–life. Five alphas and two betas are emitted in the decay chain until it decays to Lead-207 (^{207}Pb) [12]. But these radioisotopes have some disadvantages in clinical usage. (^{219}Ra), that is the daughter radioisotope of (^{223}Ra), can cause an uncontrolled irradiation of healthy tissues and organs by dispersing in the body and, on the other hand, betas emitted from these alphas emitters are a disadvantage because of the possibility of resistance mechanism to radiation therapy of betas [8].

One of the most important parameter for the radioisotope production at cyclotrons is the reaction cross–section, where nuclear reaction is likely to occur. The reaction cross–sections, as a function of energy, must be taken into account for the radioisotope production. This study is focused on the production cross–section calculations of ^{230}U. To reach the aim within the scope of this study, ^{231}Pa$(p,2n)^{230}$U, ^{231}Pa$(d,3n)^{230}$U, ^{232}Th$(p,3n)^{230}$Pa and ^{232}Th$(d,4n)^{230}$Pa reaction's cross–section calculations have been obtained by using different level density models of the TALYS 1.95 [13] code. The obtained results have been compared with the experimental data taken from the literature [14, 15] by using a relative variance analysis [16]. The most consistent level density models for each reaction have been determined by performing the relative variance analysis. After that, the total activity and the reaction yield computations have been done by using the determined most consistent level density models.

2. MATERIALS AND METHODS

One of the most basic statistical properties of the excited nucleus is the one known as level density. The first known definition of the level density was obtained by Bethe with a statistical approach for a gas consisting of non-interacting fermions [17]. This derived analytical expression is for the total level density and it was constructed where single particle levels are equally spaced and nondegenerate. Also, this model represents only the zeroth order approximation of a Fermi gas [18]. After Bethe put forward his approach, many studies have been done on this subject

and many arrangements have been proposed on this model.

However, the Fermi Gas Model (FGM) has been shown as the model known as the primary level density model, which is used in deriving all other phenomenological models. According to the fundamental approach of this model, protons and neutrons are at the lowest energy level and occupy the energy level here. It is possible for them to occupy higher energy levels only if they are excited. With this approach, the model provided successful results at low energies, but the inconsistency increased with the increase in the energy. In order to eliminate that inconsistency, it was proposed to divide the energy into two regions, low and high, and adopt a constant temperature approach. The model in which these recommendations were presented is known as the Constant Temperature Fermi Gas Model (CTFGM). The basic approach in CTFGM was to apply the constant temperature law in the region from 0 MeV to matching energy, while using the FGM for energies higher than the matching energy [19]. As a result of further studies, another model was developed and put forward in which the pairing energy is used as an arrangeable parameter and FGM can be applied at all low energies up to 0 MeV. Later, this model was named as Back-Shifted Fermi Gas Model (BSFGM) [20]. In addition to all these described models, another important model that can yield significant results is the Generalised Superfluid Model (GSM). The difference of this model from the previously described models is the way it is characterized. GSM is characterized by a phase transition from the low-energy super-fluid behavior region, where superconductivity correlations exist, to the high-energy region defined by the FGM [21].

In the calculations, CTFGM, BSFGM and GSM have been selected as the level density models. Two-Component Exciton Model has been used in the cross–section calculations. In Two-Component Exciton Model nuclear state is characterized by the sum of the total energy at any given moment during the reaction and the number of particles (p) above the Fermi surface and holes (h) below it. In this model, all possible paths for sharing the excitation energy between different particle-hole states with the same number of excitons (n=p+h) are assumed to have equal probability. The calculations of all the models mentioned and used in this study were performed with the TALYS 1.95 code [13]. TALYS is an open source package program that allows many calculations related to nuclear reactions to be made by changing various parameters such as level density models, gamma-ray strength functions, optical model potentials etc. TALYS has become one of the most preferred calculation tool in many studies in the literature due to its accuracy, consistency and the flexibility it gives the user to examine on different parameters. In this context, it is possible to show many studies in the literature comparing the theoretical results obtained by using TALYS 1.95 and other reaction codes with the experimental data [22–28].

3. RESULTS AND DISCUSSION

In this study, the production cross–section calculations of ^{230}U have been investigated. Different production routes, which are ^{231}Pa$(p,2n)^{230}$U, ^{231}Pa$(d,3n)^{230}$U, ^{232}Th$(p,3n)^{230}$Pa and ^{232}Th$(d,4n)^{230}$Pa, have been examined by using the phenomenological level density models. Relative variance analysis have been employed in order to determine the most consistent level density models. In addition to the cross–section calculations, where the obtained calculation results have been compared with the experimental data in Figs. 1–4, the activity and the reaction yields of produced radioisotopes have been computed by using the determined most consistent level density models. Also, the relative variance analysis and the optimum beam energies to produce ^{230}U and ^{230}Pa have been presented in Table 1.

The comparison of ^{231}Pa$(p,2n)^{230}$U reaction cross–section calculations with the experimental data of Morgenstern et al., [29] have been given in Figure 1. In the EXFOR [14, 15] database there is one experimental data for ^{231}Pa$(p,2n)^{230}$U reaction. Theoretical results have a shift towards to the left with respect to the experimental data. It is thought that, the experimental errors are one of the reason of this shift in addition to the differences arising from the theoretical models. Experimental data achieved maximum cross–section value, which is 33.2 ± 5.3 mb, at 14.6 MeV. The energy threshold of this reaction is 7.075 MeV but the experimental data starts at 10.6 MeV. According to the statistical analysis given in Table 1, the BSFGM is determined as the most consistent level density model among all options. Maximum cross–section value of BSFGM is 26.26 mb at 12.8 MeV proton energy. The activation and the reaction yield calculations, have been performed by using the BSFGM and 12.8 MeV beam energy. After the irradiation of 24 hours, the total activity has been found as 1.98 GBq, whereas the reaction yield has been found as 0.085 GBq/mAh.

In Figure 2, ^{231}Pa$(d,3n)^{230}$U reaction cross–section calculations versus the experiments of Morgenstern et al., [30] have been presented. In this reaction, as in the first reaction examined in the study, it is seen that there are differences between the experimental data and the theoretical calculation

Table 1. Relative variance results with beam energy

Reaction	CTFGM	BSFGM	GSM	Beam Energy (MeV)
^{231}Pa$(p, 2n)^{230}$U	1.3443	0.7474	0.8368	12.8
^{231}Pa$(d, 3n)^{230}$U	0.4250	0.6636	0.60	17.9
^{232}Th$(p, 3n)^{230}$Pa	1.7564	1.2208	0.3940	21.5
^{232}Th$(d, 4n)^{230}$Pa	2.3203	0.7212	0.4843	37.94
Total Variance	5.85	3.35	2.32	

results due to the differences in the computational dynamics of the theoretical models. Nevertheless, as can be seen in Figure 2 and Table 1, the CTFGM is found as the most consistent level density model. The reaction cross–section value for the CTFGM at 17.9 MeV has been found as 32.78 mb. According to this result, the level density model has been fixed to the CTFGM then the reaction yield and the activation calculations have been done for the 17.9 MeV beam energy. The maximum activity has been found as 2.21 GBq whereas the maximum reaction yield has been found as 0.094 GBq/mAh.

^{232}Th$(p, 3n)^{230}$Pa reaction cross–section calculations versus the experimental data of Morgenstern et al. [29] and Jost et al. [31] have been given in Figure 3. The CTFGM and the BSFGM have produced higher cross–section results than the experimental data. The GSM is determined the most consistent level density model with 0.3940 relative variance value. Unsurprisingly, there are differences between theoretical models, that calculate using different parameters, and experimental data obtained from the literature. The proton beam energy has been selected as 21.5 MeV for the reaction yield and the activation calculations, which were carried out by selecting the GSM as the level density model. The maximum activity is calculated as 52 GBq after the irradiation of 24 hours, whereas the maximum yield is 2.21 GBq/mAh.

^{232}(p,3n) reaction are an order of magnitude greater than the cross sections for the ^{231}Pa$(p, 2n)$ reaction. Standartly, the probability of 3 neutron emission is lower than 2 neutron emission, but target materials are different in these reactions. In this study, the energies of projectile particles are in the compound reaction energy region. Compound nuclei of these reactions are ^{233}Pa (odd–odd) and ^{232}U (even–even). So pairing nucleons of the compound nuclei may be the reason for this result.

The reaction cross–section calculations of ^{232}Th$(d, 4n)^{230}$Pa reaction have been given in Figure 4. Knowing that the calculation results obtained by utilizing the theoretical models which have different algorithms will not be fully compatible with the experimental data, the experimental data of Duchemin et al. [32] and Rao et al. [33] have been used to

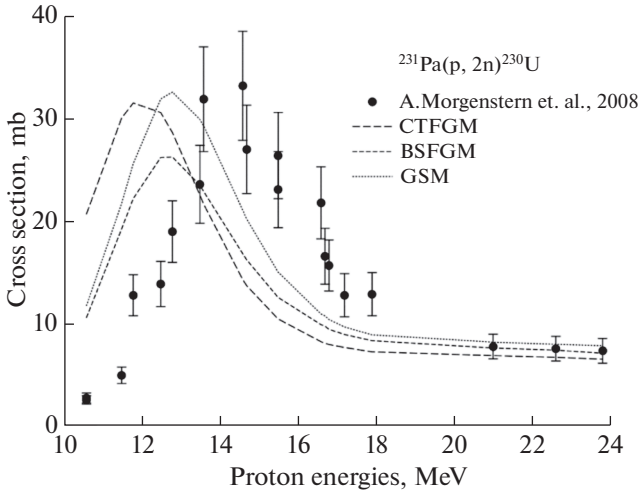


Fig. 1. Comparisons of ^{231}Pa$(p, 2n)^{230}$U reaction cross–section calculations with experimental data.

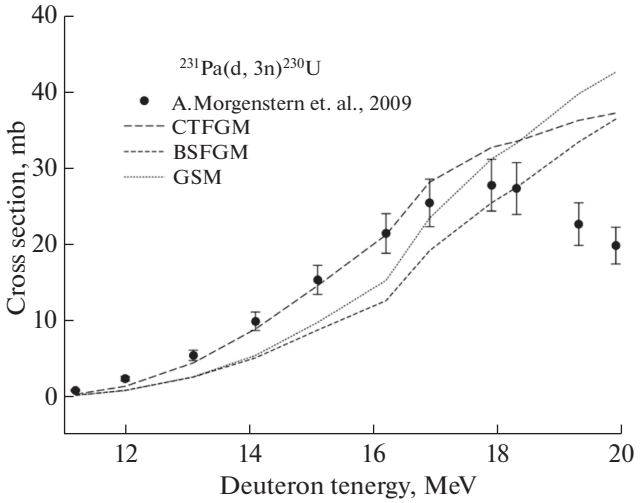


Fig. 2. Comparisons of ^{231}Pa$(d, 3n)^{230}$U reaction cross–section calculations with experimental data.

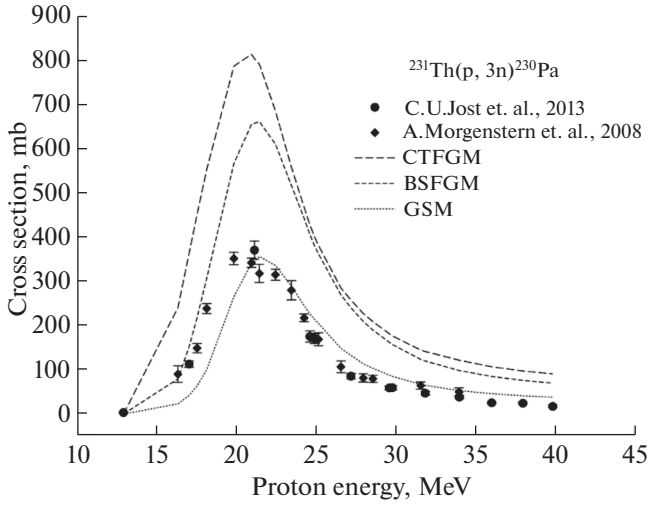


Fig. 3. Comparisons of $^{232}\mathrm{Th}(p,3n)^{230}\mathrm{Pa}$ reaction cross–section calculations with experimental data.

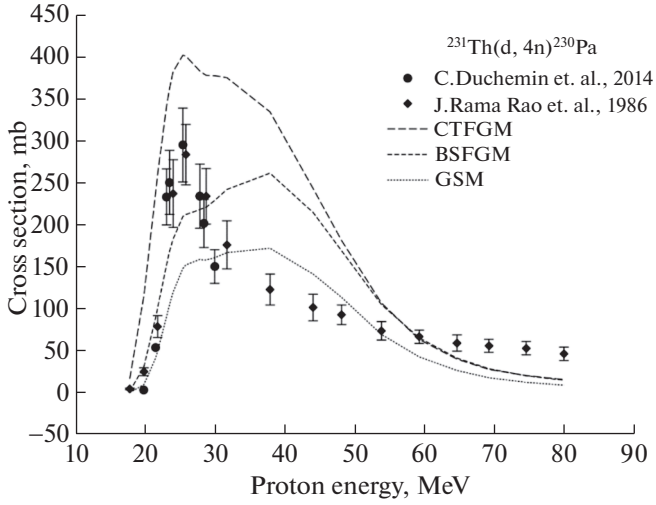


Fig. 4. Comparisons of $^{232}\mathrm{Th}(d,4n)^{230}\mathrm{Pa}$ reaction cross–section calculations with experimental data.

determine which theoretical model calculation results are most compatible with the experimental data. According to the relative variance analyses given in Table 1, the GSM has been found as the most consistent level density model. The beam energy has been selected as 37.94 MeV for the activity and the reaction yield calculations. The maximum activity and the maximum yield have been determined as 44.63 GBq and 1.9 GBq/mAh, respectively.

The thickness of the target material was calculated by using monte carlo based SRIM 2013 code [34]. The thickness was obtained 39.72 μm for 12.00 MeV and 44.77 μm for 13.00 MeV for the target. Also surface areas of target were selected 10 cm^2 at TALYS 1.95 code.

Considering the calculation results and experimental data obtained with the theoretical models on the basis of the reactions examined, it can be said that the results produced by the use of theoretical models are generally consistent with which researchers can obtain a prediction. Another point to be noticed, when examined carefully, is that, although only one neutron output occurs in the reactions of interest, when switching from the ^{231}Pa target to the ^{232}Th target, there are nearly ten–fold changes in the cross–section values. One of the reasons for this situation can be shown as the change of the target and so the differences in the reaction processes experienced in the context of target, incident particle and incident particle energy involved into the theoretical calculations.

On the other hand, it is known that the decay of ^{230}Pa to ^{230}U via β^- is 7.8% possibility [35]. In addition to the small possibilities, the bigger cyclotrons are needed for the production routes involving ^{230}Pa. The beam energies have been found as 12.8, 17.9, 21.5 and 37.94 MeV for $^{231}\mathrm{Pa}(p,2n)^{230}\mathrm{U}$, $^{231}\mathrm{Pa}(d,3n)^{230}\mathrm{U}$, $^{232}\mathrm{Th}(p,3n)^{230}\mathrm{Pa}$, $^{232}\mathrm{Th}(d,4n)^{230}\mathrm{Pa}$, respectively. Considering the findings above mentioned, $^{231}\mathrm{Pa}(p,2n)^{230}\mathrm{U}$ is found as the best production route to obtain ^{230}U. After the determining the best production route, the maximum activities for the different irradiation times at 1 mA beam current have been given in Table 2.

Calculations in this study present the main reactions of interest to produce ^{230}U. However, the cyclotron irradiations also produce many other products that might be highly undesirable. Thus, some additional calculations have been performed to determine the relative production of these undesirable isotopes for the $^{231}\mathrm{Pa}(p,2n)^{230}\mathrm{U}$ reaction at 12.8 MeV incident proton energy. In these calculations, it was found that, in addition to the main product of ^{230}U (23% of total product) with 0.085 GBq/mAh, ^{231}U with a yield of 0.285 GBq/mAh (about 77% of total product) and various other products with trace amounts were formed (^{223}Ra, ^{224}Ra, ^{225}Ra, ^{225}Ac, ^{226}Ac, ^{227}Ac, ^{226}Th, ^{227}Th, ^{228}Th, ^{230}Th, ^{230}Pa, $^{232}\mathrm{U} < 10^{-8}$ GBq/mAh). Although it is possible to chemically separate other available undesirable products as traces amount in this total product (exception of ^{232}U) after irradiation, it is not possible to separate ^{231}U from ^{230}U by chemical method [36]. Thus, ^{230}U can be used after the amount of ^{231}U with 4.2 days decay time has been reduced to an acceptable

Table 2. Maximum activity for different irradiation times and beam currents

Beam Current	Maximum activity after 1 hour irradiation GBq (mCi)	Maximum activity after 4 hours irradiation GBq (mCi)	Maximum activity after 12 hours irradiation GBq (mCi)	Maximum activity after 24 hours irradiation GBq (mCi)
1.000 mA	0.0838 (2.2648)	0.3345 (9.0405)	0.9978 (26.967)	1.9792 (53.491)

level (at least below 1%) with an appropriate waiting time.

Undesirable radioisotope ^{231}U decays to ^{231}Pa by electron capture at a possibility of 100%. Since ^{231}Pa is already the target material in this direct production route, ^{231}Pa obtained from undesirable product ^{231}U can be stored and processed for re-use as the target material. In this way, a significant amount of source material can be recovered.

Friend et al., [37] have investigated the ^{230}U production and determined that the ^{232}Th$(p, 3n)^{230}$Pa indirect reaction is the best route and they recommend a 28 days waiting time for enough ^{230}U production from ^{230}Pa. After this waiting time, relative remaining production ratio of ^{230}U in indirect route decreases from 7.8% to 3.12%. In our study for a waiting time as their suggested, in 28 days after production, the amount of undesirable ^{231}U in total product decreases from 77% to 0.76% (less than 1%). Of course, after 28 days waiting time, remaining relative production ratio of ^{230}U in direct route decreases from 23% to 9.06%. However, this amount of main product ^{230}U in direct route recommended by this study is still relatively 3 times higher than the amount of main product ^{230}U to be obtained by indirect route.

As can be seen in Table 2, it is possible to produce an ^{230}U activity of 53.491 mCi via on ^{231}Pa$(p, 2n)^{230}$U direct route with 12.8 MeV protons at 1 mA current for 24 hours. After a 28 days waiting period required for undesirable product (^{231}U) activity to decrease sufficiently, this activity decreases to 21.4 mCi. Treatment dose can be up to 200 mCi in the targeted beta therapy [3] whereas very low dose changed between 0.1 and 1 mCi are applied in the TAT [38]. By considering the average dose per patient as 0.5 mCi, these activities are enough for 43 patients. This is a satisfying amount in terms of the number of patients treated in clinics, and unlike the generator production, cyclotron production can be made every day.

4. SUMMARY AND CONCLUSION

The obtained results in this study can be summarized as follows.

Generally, reaction cross–section calculation results obtained by utilizing the possible level density models are consisted with the experimental data which are taken from EXFOR [14, 15] database. As can be seen from the last column of Table 1, the GSM is found as the most consistent level density model for reactions investigated in this paper. When the results are evaluated by considering the reactions examined in this study, it is seen that the models in which the most compatible results with the experimental data differ. Some of the reasons for this situation can be shown as the theoretical models use different parameters in the calculations, the calculation algorithms they follow are different, and the differences that may occur in the reaction mechanisms depending on the target and the projectile and its energy.

The beam energy for production of the ^{230}U, are determined as 12.8 MeV, 17.9 MeV, 21.5 MeV, and 37.9 MeV for the ^{231}Pa$(p, 2n)^{230}$U, ^{231}Pa$(d, 3n)^{230}$U, ^{232}Th$(p, 3n)^{230}$Pa and ^{232}Th$(d, 4n)^{230}$Pa reactions, respectively.

It is extremely important to provide an appropriate target in radioisotope production. In addition, it should not be forgotten that the target availability, machinability, sustainability and cost are extremely critical for medical applications. Even though developing technology and advancing scientific applications are conducive to changes in such parameters, attention should be paid to such issues as well. In this context, it should also be noted that protactinium is not a stable element. ^{231}Pa is an alpha emitter with a half-life of 32.780 years. Emitted alpha rays from ^{231}Pa can be stopped easily and it is possible to produce a target in a suitable form using ^{231}Pa by taking appropriate radiation protection measures [39]. However, the low amount of ^{231}Pa in nature is a significant problem. One of the solution to this problem could be the separation of ^{231}Pa from ^{235}U, which is one of the most abundant radioactive element in nature. ^{231}Pa is present in natural Uranium with ^{235}U at a rate of 0.34 mg/kg [40]. However, this ratio is insufficient to obtain an adequate amount of ^{231}Pa. On the other hand, ^{232}Th is another radioisotope that has the most abundance rate in nature and it is possible to obtain the ^{231}Pa in the desired amount

via the ^{232}Th(n,2n)^{231}Th ($^{231}Th \xrightarrow{\beta^-} {}^{231}$Pa) ^{231}Pa; $T_{1/2} = 25.5$ h) reaction using neutrons in the nuclear reactors [41].

In addition to above production methods of ^{231}Pa, the initial ^{231}Pa target can be recovered up to 76% via on undesirable products (^{231}U) of direct route. This radioactive recycling is extremely valuable in terms of both the supply of ^{231}Pa and the prevention of radioactive pollution from long–lived radioactive elements, such as ^{231}Th ($t_{1/2} = 75.400$ year) occured from indirect route. In addition to these advantages, the direct reaction route proposed in this study significantly reduces the cyclotron cost by reducing the cyclotron requirement from 21.5 MeV to 12.8 MeV.

REFERENCES

1. D. V. Becker and C. T. Sawin, "Radioiodine and thyroid disease: The beginning," Semin. Nucl. Med. **26**, 155–164 (1996). https://doi.org/10.1016/S0001-2998(96)80020-1
2. A. S. Shah, Hameedullah, S. Farrukh, K. A. Shah, A. U. Khan, and M. R. Khattak, "Radiation doses from ^{131}I treated hyperthyroidism patients versus life style: A survey," Int. J. Radiat. Res. **13**, 67–72 (2015).
3. J. Graf, U.-F. Pape, H. Jann, T. Denecke, R. Arsenic, W. Brenner, M. Pavel, and V. Prasad, "Prognostic significance of somatostatin receptor heterogeneity in progressive neuroendocrine tumor treated with Lu-177 DOTATOC or Lu-177 DOTATATE," Eur. J. Nucl. Med. Mol. Imaging **47**, 881–894 (2020). https://doi.org/10.1007/s00259-019-04439-9
4. J. Kunikowska and L. Królicki, "Targeted α-emitter therapy of neuroendocrine tumors," Semin. Nucl. Med. **50**, 171–176 (2020). https://doi.org/10.1053/j.semnuclmed.2019.11.003
5. J. G. Jurcic, S. M. Larson, G. Sgouros, M. R. McDevitt, R. D. Finn, C. R. Divgi, A. M. Ballangrud, K. A. Hamacher, D. Ma, J. L. Humm, M. W. Brechbiel, R. Molinet, and D. A. Scheinberg, "Targeted alpha particle immunotherapy for myeloid leukemia," Blood **100**, 1233–1239 (2002). https://doi.org/10.1182/blood.V100.4.1233.h81602001233_1233_1239
6. A. F. Maaland, A. Saidi, J. Torgue, H. Heyerdahl, T. A. R. Stallons, A. Kolstad, and J. Dahle, "Targeted alpha therapy for chronic lymphocytic leukaemia and non-Hodgkin's lymphoma with the anti-CD37 radioimmunoconjugate ^{212}Pb-NNV003," PLoS One **15**, 0230526 (2020). https://doi.org/10.1371/journal.pone.0230526
7. G. Sgouros, J. C. Roeske, M. R. McDevitt, S. Palm, B. J. Allen, D. R. Fisher, A. B. Brill, H. Song, R. W. Howell, G. Akabani, SNM MIRD Committee; W. E. Bolch, A. B. Brill, D. R. Fisher, R. W. Howell, R. F. Meredith, G. Sgouros, B. W. Wessels, and P. B. Zanzonico, "MIRD Pamphlet No. 22 (abridged): Radiobiology and dosimetry of alpha-particle emitters for targeted radionuclide therapy," J. Nucl. Med. **51**, 311–328 (2010). https://doi.org/10.2967/jnumed.108.058651
8. M. A. Walicka, G. Vaidyanathan, M. R. Zalutsky, S. J. Adelstein, and A. I. Kassis, "Survival and DNA damage in Chinese hamster V79 cells exposed to alpha particles emitted by DNA-incorporated astatine-211," Radiat. Res. **150**, 263–268 (1998). https://doi.org/10.2307/3579974
9. WHO-2014, Our Planet, Our health, Report of the WHO Comission on health and Environment World Health Organization, Geneva, 2 (1992). `http://www.who.int/en/`.
10. Nuclear Data. `http://nucleardata.nuclear.lu.se/toi/nuclide.asp?iZA=920230`. Cited March 2021.
11. J. L. Hatcher-Lamarre, V. A. Sanders, M. Rahman, C. S. Cutler, and L. C. Francesconi, "Alpha emitting nuclides for targeted therapy," Nucl. Med. Biol. **92**, 228–240 (2021). https://doi.org/10.1016/j.nucmedbio.2020.08.004
12. A. E. Brito and E. Etchebehere, "Radium-223 as an approved modality for treatment of bone metastases," Semin. Nucl. Med. **50**, 177–192 (2020). https://doi.org/10.1053/j.semnuclmed.2019.11.005
13. A. Koning, S. Hilaire and S. Goriely, *TALYS-1.95 A Nuclear Reaction Program, User Manual* (NRG, The Netherlands, 2019).
14. N. Otuka, E. Dupont, V. Semkova, B. Pritychenko, A. I. Blokhin, M. Aikawa, S. Babykina, M. Bossant, G. Chen, S. Dunaeva, R. A. Forrest, T. Fukahori, N. Furutachi, S. Ganesan, Z. Ge, O. O. Gritzay, M. Herman, S. Hlavac, K. Kato, B. Lalremruata, Y. O. Lee, A. Makinaga, K. Matsumoto, M. Mikhaylyukova, G. Pikulina, V. G. Pronyaev, A. Saxena, O. Schwerer, S. P. Simakov, N. Soppera, R. Suzuki, S. Takacs, X. Tao, S. Taova, F. Tarkanyi, V. V. Varlamov, J. Wang, S. C. Yang, V. Zerkin, and Y. Zhuang, "Towards a more complete and accurate experimental nuclear reaction data library (EXFOR): International collaboration between nuclear reaction data centres (NRDC)," Nucl. Data Sheets **120**, 272–276 (2014). https://doi.org/10.1016/j.nds.2014.07.065
15. V. V. Zerkin and B. Pritychenko, "The experimental nuclear reaction data (EXFOR): Extended computer database and Web retrieval system," Nucl. Instrum. Methods Phys. Res., Sect. A **888**, 31–43 (2018). https://doi.org/10.1016/j.nima.2018.01.045
16. N. V Kurenkov, V. P Lunev, and Yu. N Shubin, "Evaluation of calculation methods for excitation functions for production of radioisotopes of iodine, thallium and other elements," Appl. Radiat. Isot. **50**, 541–549 (1999). https://doi.org/10.1016/S0969-8043(98)00048-7
17. H. Bethe, "An attempt to calculate the number of energy levels of a heavy nucleus," Phys. Rev. **50**, 332 (1936). https://doi.org/10.1103/PhysRev.50.332

18. V. Paar and R. Pezer, "Generalized Bethe formula for the total level density," Phys. Rev. C **55**, R1637 (1997).
https://doi.org/10.1103/PhysRevC.55.R1637
19. A. V. Ignatyuk, K. K. Istekov, and G. N. Smirenkin, "The role of collective effects in the systematics of nuclear level densities," Sov. J. Nucl. Phys. **29**, 450 (1979).
20. H. Baba, "A shell-model nuclear level density," Nucl. Phys. A bf 159, 625–641 (1970).
https://doi.org/10.1016/0375-9474(70)90862-6
21. A. V. Ignatyuk, G. N. Smirenkin, and A. S. Tishin, "Phenomenological description of the energy dependence of the level density parameter," Sov. J. Nucl. Phys. **21**, 255 (1975).
22. M. Sadeghi, M. Aboudzadeh, A. Zali, and B. Zeinali, "^{86}Y production via ^{86}Sr(p,n) for PET imaging at a cyclotron," Appl. Radiat. Isot. **67**, 1392 (2009).
https://doi.org/10.1016/j.apradiso.2009.02.038
23. M. Sadeghi, T. Kakavand, and Z. Alipoor, "^{85}Sr Production via proton induced on various targets using Talys 1.0 code," Mod. Phys. Lett. A **25**, 1541–1552 (2010).
https://doi.org/10.1142/S0217732310032615
24. O. Karaman, H. Özdoğan, Y. A. Üncü, C. Karaman, and G. Tanır, "Investigation of the effects of different composite materials on neutron contamination caused by medical LINAC," Kerntechnik **85**, 401–407 (2020).
https://doi.org/10.3139/124.200022
25. S. M. Qaim, "Nuclear data for production and medical application of radionuclides: Present status and future needs," Nucl. Med. Biol. **44**, 31–49 (2017).
https://doi.org/10.1016/j.nucmedbio.2016.08.016
26. T. Bitam and M. Belgaid, "Newly developed semi-empirical formulas of nuclear excitation functions for (n,α) reactions at the energy range $12 \leq E_n \leq 20$ MeV and mass number range $30 \leq A \leq 128$," Nucl. Phys. A **991**, 121614 (2019).
https://doi.org/10.1016/j.nuclphysa.2019.121614
27. L. Yettou and M. Belgaid, "Calculation of pre-equilibrium effects in neutron-induced cross section on ^{32,34}S isotopes using the EMPIRE 3.2 code," EPJ Web Conf. **100**, 01009 (2015).
https://doi.org/10.1051/epjconf/201510001009
28. H. Özdoğan, Y. A. Üncü, M. Şekerci, and A. Kaplan, "Estimations of giant dipole resonance parameters using artificial neural network," Appl. Radiat. Isot. **169**, 109581 (2021).
https://doi.org/10.1016/j.apradiso.2020.109581
29. A. Morgenstern, O. Lebeda, J. Stursa, F. Bruchertseifer, R. Capote, J. Mcginley, G. Rasmussen, M. Sin, B. Zielinska, and C. Apostolidis, "Production of ^{230}U/^{226}Th for targeted alpha therapy via proton irradiation of ^{231}Pa," Anal. Chem. **80**, 8763–8770 (2008).
https://doi.org/10.1021/ac801304c
30. A. Morgenstern, O. Lebeda, J. Stursa, R. Capote, M. Sin, F. Bruchertseifer, B. Zielinska, and C. Apostolidis, "Cross sections of the reaction ^{231}Pa$(d,3n)^{230}$U for the production of ^{230}U/^{226}Th for targeted alpha therapy," Phys. Rev. C **80**, 054612 (2009).
https://doi.org/10.1103/PhysRevC.80.054612
31. C. U. Jost, J. R. Griswold, S. H. Bruffey, S. Mirzadeh, D. W. Stracener, and C. L. Williams, "Measurement of cross sections for the ^{232}Th(p,4n)^{229}Pa reaction at low proton energies," AIP Conf. Proc. **1525**, 520 (2013).
https://doi.org/10.1063/1.4802383
32. C. Duchemin, A. Guertin, F. Haddad, N. Michel, and V. Metivier, "^{232}Th(d,xn)^{230,232,233}Pa cross section measurements," Nucl. Data Sheets **119**, 267–269 (2014).
https://doi.org/10.1016/j.nds.2014.08.073
33. J. R. Rao, J. Ernst, and H. Machner, "Comparative study of d- and ^{6}Li-induced reactions on ^{232}Th in terms of breakup and preequilibrium processes," Nucl. Phys. A **448**, 365–380 (1986).
https://doi.org/10.1016/0375-9474(86)90097-7
34. J. F. Ziegler, M. D. Ziegler, and J. P. Biersack, "SRIM—The stopping and range of ions in matter (2010)," Nucl. Instrum. Methods Phys. Res., Sect. B **268**, 1818–1823 (2010).
https://doi.org/10.1016/j.nimb.2010.02.091
35. NUDAT. `https://www.nndc.bnl.gov/nudat2/`. Cited March, 2021.
36. T. Mastren, A. Akin, R. Copping, M. Brugh, D. S. Wilbur, E. R. Birnbaum, F. M. Nortier, K. D. John, and M. E. Fassbender, "A reverse ^{230}U/^{226}Th radionuclide generator for targeted alpha therapy applications," Nucl. Med. Biol. **90–91**, 69–73 (2020).
https://doi.org/10.1016/j.nucmedbio.2020.09.006
37. M. T. Friend, T. Mastren, T. G. Parker, C. E. Vermeulen, M. Brugh, E. R. Birnbaum, F. M. Nortier, and M. E. Fassbender, "Production of ^{230}Pa by proton irradiation of ^{232}Th at the LANL isotope production facility: Precursor of ^{230}U for targeted alpha therapy," Appl. Radiat. Isot. **156**, 108973 (2020).
https://doi.org/10.1016/j.apradiso.2019.108973
38. J. Dahle, J. Borrebaek, T. J. Jonasdottir, A. K. Hjelmerud, K. B. Melhus, Ø. S. Bruland, O. W. Press, and R. H. Larsen, "Targeted cancer therapy with a novel low-dose rate alpha-emitting radioimmunoconjugate," Blood **110**, 2049–2056 (2007).
https://doi.org/10.1182/blood-2007-01-066803
39. P. S. Morrall, "Target preparation method and characterisation," Nucl. Instrum. Methods Phys. Res., Sect. B **613**, 423–424 (2010).
https://doi.org/10.1016/j.nima.2009.09.091
40. A. A. Dalvi and R. Verma, "Radiochemicalseparation of ^{231}Pa from siliceous cake prior to its determination by gamma ray spectrometry," Radiochim. Acta **105**, 831–839 (2017).
https://doi.org/10.1515/ract-2017-2776

41. T. Imamura, M. Saito, T. Yoshida, and V. Artisyuk, "Production of Pa–U fuel with proliferation resistance by 14 MeV neutron for long-life core, J. Nucl. Sci. Technol. **41**, 655–664 (2004).

https://doi.org/10.1080/18811248.2004.9715530